



Comparison of optical and photocatalytic properties of TiO₂ thin films modified with Ag nanoparticles

H.R.Ravi^{1*}, P.N.Prashanth kumar², H.R.Sreepad³

¹Research centre, PG Department of physics, BETAHE, Bharthinagara, Mandya, (INDIA)

²Department of Industrial Chemistry, Kuvempu University, Shankaraghatta-577 451, (INDIA)

³Research centre, PG Department of physics, GFG College, Mandya, (INDIA)

E-mail: ravihr1@yahoo.co.in

ABSTRACT

This paper describes the development of nano structured Ag-TiO₂ thin films by exposure of Ag⁺ ions on anatase phased TiO₂ films by microwave glycol irradiation. It was characterized by XRD, SEM, EDX and XPS confirmed that films were anatase phase having uniform morphology and their optical characterization showed a shift in optical absorption towards shorter wavelength, which was correlated with the structural variation of the silver ions deposited on TiO₂ thin film. In order to test them the photocatalytic degradation of MB as a standard analysis. The absorbance intensity of the organic pollutants decreases which was related to associate effects: the electron transfer from TiO₂ to Ag and reducing the electron-hole recombination. Hence this paper we compared that Optical and photocatalytic properties of EBE and SGD films from the UV-Visible absorbance spectrophotometer. The result shows that without surfactant SGD Ag-TiO₂ and EBE Ag-TiO₂ films exhibited much better photoactivity than the surfactant SGD Ag-TiO₂ films due to excess of silver composition on surfactant SGD-TiO₂ films this has been explained in terms of the EDX Analysis. © 2016 Trade Science Inc. - INDIA

KEYWORDS

TiO₂ film;
Ag-TiO₂ film;
Methylene blue;
Photocatalyst.

INTRODUCTION

Contaminated water and polluted air have affected the environment and human health seriously; hence, much research has been undertaken to address this global issue. However, the publication in 1971 of the work by *Formenti et al.*,^[1] followed one year later by *A. Fujishima* and *K. Honda*'s^[2] renowned article prompted a true revolution based on the extensive use of TiO₂ as a unique photocatalyst. Ever

since this decade interest in this semiconductor was first in academia and then in industry, has grown exponentially. During this time, photocatalysis with TiO₂ was applied with varied success to a number of processes, including hydrogen production, effluents detoxication and disinfection, and organic synthesis^[3-8]. The relatively high quantum yield and elevated stability of TiO₂ are the key reasons for the preponderance of this semiconductor, which has become a virtual synonym for photocatalyst. Now a

Full Paper

days, photocatalytic coatings deposited on external building elements, like windows, along with air purifiers are the main products of this emerging business, but dozens of other commercial uses have been proposed and some experimental devices are already on the market^[9–11]. Despite these achievements and remarkable advantages, heterogeneous photocatalysis with TiO₂ has to cope with significant limitations. In general, photocatalytic reaction rates are moderate and consequently this technology is not appropriate for high throughput processes, as an example in the decontamination of heavily polluted industrial effluents^[4, 5, 12]. Increment of photon flux increases the reaction rate, but saturation is usually achieved at relatively low irradiance and energetic efficiency of the process drops consequently^[12, 13].

However, the most important drawback of photocatalysis is derived from mismatch between the TiO₂ band gap energy and the sunlight spectra, which overlap only in the UVA (400–320 nm) and UVB (320–290 nm) ranges. As a consequence, this technology can only take advantage of less than 6% of the solar energy impinging on the earth's surface and its potential as a sustainable technology cannot be entirely fulfilled^[8–13]. This fact has profoundly influenced research in photocatalysis, so that modification of TiO₂ to achieve efficient photoactivation in the visible spectrum is an active field of research^[3–8, 14, 15]. During the last few years an increasingly great number of new photocatalysts have been synthesized and tested as possible alternatives to TiO₂. These materials are derived from TiO₂ by any of the usual modifications such as doping, coupling with an additional phase, or morphological changes, the ability to either change band gap of titania to allow photoactivity on irradiation with visible light or to decrease the electron/hole recombination rate is being pursued. Many efforts have been attempted by modification of titanium dioxide with metal-ion implanted TiO₂ (using transition metals: Cu, Co, Ni, Cr, Mn, Mo, Nb, V, Fe, Ru, Au, Ag, Pt)^[16–18], reduced TiOx photocatalysts^[19–20] non-metal doped-TiO₂ (N, S, C, B, P, I, F)^[21–23] composites of TiO₂ with semiconductor having lower band gap energy (e.g. CdS particles)^[24].

The deposited noble metals on the surface of

TiO₂ can not only act as traps to capture the photoinduced electrons and holes, leading to the reduction of electron hole recombination in photocatalytic processes, but also act to increase the absorption capability for visible light due to the surface plasmon resonance (SPR) effect of noble metals. Specially loading of noble metal such as Au and Ag can absorb visible light *via* surface plasmon resonance (SPR) to enhance photocatalytic activity^[25–28]. In simple terms, SPR is collective oscillations of conduction band electrons in a metal particle driven by the electromagnetic field of incident light^[29]. However, some noble metals such as Pt, Pd, Rh, and Au are too expensive to be used in industrial applications. Recently Ag NPs also show a very intense localized surface plasmon absorption in the near-UV region^[30], which greatly enhances the electric field intensity in the vicinity of the Ag NPs. This enhanced near field at near-UV region could increase the light absorption to boost the excitation of electron-hole pairs in TiO₂ and thus increase the efficiency of photocatalysis. This clearly indicates that the LSPR^[31] effect is a potential way for the enhancement of photocatalysis.

Thus, the research of Ag-modified TiO₂ shows more significant practical value when Ag-TiO₂ materials are considered as photocatalysis. The preparation methods of the composite material play an important role in determining the photocatalytic activity. The distribution of metals and the interaction between the dopant and TiO₂ support are noticeably dependent on preparation methods. A variety of synthesis approaches have been carried out to prepare titania materials. The widely used methods include, vacuum techniques such as chemical vapor deposition^[32], Electron beam vaporization^[34] and alkoxide sol-gel process^[33] which are emerged as one of the most promising techniques for growing TiO₂ thin films. The TiO₂ thin films prepared by alkoxide sol-gel method can be of high purity and low cost due to availability of high purity chemicals and the simplicity of process. It is one of the most popular techniques used for fabrication of TiO₂ thin films modified by metal ions, which were uniformly modified in thin film for most of studies. The prepared all titania films were exposed to silver ions

by simple microwave glycol reduction technique to prepare silver doped TiO_2 films. Many researchers reported that Ag- TiO_2 prepared by a photodeposition method will make Ag highly dispersed on the surface of TiO_2 and increase the photo efficiency^[35]. However, the impregnation method are simple and without usage of UV light irradiation^[36].

Thus, it is worthy to compare these methods and to investigate the relationship between preparation methods and corresponding photoactivity. The purpose of this chapter is to assess the feasibility of microwave glycol reduction technology to improve the photo-catalysis and optical efficiencies of TiO_2 thin films by Ag ion implantation. The obtained results presented here may assist in understanding the phenomena involved for photocatalytic degradation of pollutants using immobilized materials supported as thin films. Several researchers have synthesized Ag- TiO_2 sol by adding silver compound to modify the sol-gel process^[37], Bin Zhao *et al.* prepared the Ag- TiO_2 nanocomposites by photoreduction method, which requires 2h UV-irradiation to in-situ reduce Ag^+ ions on the surface of TiO_2 leading to Ag- TiO_2 composite nanoparticles (NPs)^[38]. Li, X.; Wang *et al.* reported about microwave irradiation method for the preparation of Ag- TiO_2 nano particles^[39]. Feng Peng *et al.* reported the preparation of Ag-sensitized ZnO nanoparticles by microwave reduction method^[36]. To the best of author's knowledge, not much of work have been cited in the literature on the preparation of Ag- TiO_2 nanocomposite thin films by glycol reduction using microwave irradiation method.

EXPERIMENTAL SECTION

Materials and methods

Titanium isopropoxide (+97%) and silver nitrate (AgNO_3 , analytical grade) were purchased from Sigma Aldrich were used for the preparation of TiO_2 and Ag- TiO_2 photocatalysts. Methylene blue dye (MB) was used as target compound for degradation. For prepared MB solution double distilled deionized water was used. All the materials were AR graded materials and no needed for further purification.

Spectral measurements

The phase compositions and structures of doped and undoped semiconducting oxide samples were determined by x-ray diffraction (XRD, PANalytical Xpert Pro X-ray Diffractometer) with Cu K radiation ($k = 0.15406 \text{ nm}$). The morphology of samples were observed by scanning electronic microscopy (SEM) with a JSM-6700 LV electron microscope operating at 5.0 kV, followed by examination of chemical compositions by X-ray energy dispersive spectroscopy (EDS). The Binding energy and chemical states of composite films were characterized by X-ray photon spectroscopy (XPS). Light absorption properties of these films were studied using UV-Vis spectrophotometer (Shimadzu, UV-1650 PL model).

Preparation of TiO_2 thin films by electron beam evaporation (EBE) technique

Titanium dioxide films were deposited by reactive electron beam evaporation in a conventional deposition plant (Edwards High Vacuum Ltd., U.K.). The vacuum obtained was 5×10^{-6} Torr. The starting material TiO_2 were evaporated from a 6 kW e-beam gun (Leybold Heraeus, Germany). The rate of deposition was about 100 /min and the partial pressure of O_2 , (99.99% purity) was 2×10^{-4} Torr. The substrates were maintained at temperatures of 250°C during deposition. A Heitmann type discharge source was used to ionize the oxygen to enhance the reactivity between the evaporant and oxygen in order to get stoichiometric films. The schematic deposition of plant and other deposition conditions were described as above and the films were post heated in air for 4 h at particular temperatures (200°C).

Preparation of TiO_2 thin film by sol gel method (SGD)

Titanium tetra isopropoxide (sigma Aldrich 99.9%) has been used as the titania precursor, the matrix sol was prepared by mixing titanium tetra isopropoxide (TTIP) with absolute ethanol (Aldrich 99.9%) and acetyl acetone at room temperature. Here the absolute ethanol has been used as a solvent. Acetyl acetone has been used to control the pH of the hydrolysis/condensation reactions in sol-gel so-

Full Paper

lution The molar ratio of final composition of solution was TIP: ethanol: acetyl acetone= 1:9:0.5. The obtained sol-gel have been spin coated onto well cleaned soda lime glass substrates using the above solution. The sol was put in drops on the substrate, which was rotated at a speed of 3000 rpm for 60 s resulting in the formation of a thin film. The film was heated at 100 C for 10 min and then allowed to cool to room temperature. TiO₂ was again spin coated on the already coated TiO₂ film and heated at 100°C for 10min and then allowed to cool to room temperature. The spin coating, heating and cooling process was repeated four times in order to get desired thicker films. The films were annealed at 500° C for 1h using a heating rate of 2°C/min^[40].

Preparation of PEG-2000 surfactant TiO₂ thin films (PEG-SGD film)

By the addition of PEG-2000 surfactant followed by above procedure is used for preparation of porous TiO₂ thin films. The final composition of the solution in molar ratio was TIP: ethanol: acetyl acetone: PEG-2000 = 1: 9:0.5:0.05. Finally it was heat treated with the above procedure to get the desired thickness of thin films.

RESULT AND DISCUSSION

XRD studies

Figure (2.1 A, B and C) shows that XRD pat-

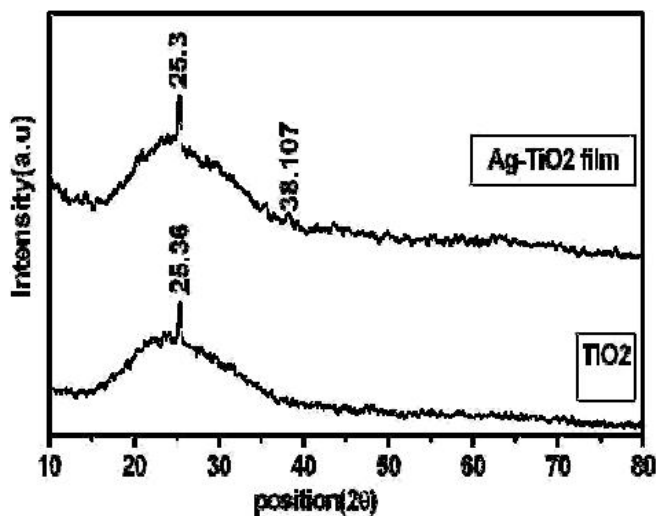


Figure 1a : Wide-angle X-ray scattering patterns of the resultant (a) EBE TiO₂ and (b) Ag-TiO₂ films

terns of TiO₂ and Ag-TiO₂ samples prepared by three different methods. There is no obvious difference among these three TiO₂ and Ag-TiO₂ samples, since all samples consist of anatase as major crystalline phase within the detection limits of this technique. In addition, there is no remarkable shift of all diffraction peaks, implying that no TiO₂-Ag_xO films are formed in all of the as-prepared samples^[41]. The average size of crystallites was estimated based on broadening of the (101) peak at $(2\theta) = 25.3^\circ$ using Scherer equation, $d = k / B \cos (2\theta)$. The crystallite size of all Ag-TiO₂ sample is smaller than that of the TiO₂ films. The small crystallite size indicates that unique sample preparation method used in the present work can effectively prompt anatase crystallization and inhibits grain growth if compared with TiO₂ films. These findings may also imply that the agglomeration of TiO₂ nanocrystallite is interrupted by deposition of silver particles on the interface of TiO₂. From the obtained XRD results it can be seen that EBE Ag-TiO₂ films shows a very small peak at 38.01 belonging to Ag which exactly matches with the JCPDS Card No. 00-004-0783. To confirm that metallic state of the silver on surface of the resultant EBE film samples, it was further characterized by XPS measurement.

The obtained particle size of different Ag-TiO₂ samples, indicate a slight influence of preparation methods on the textual properties of Ag-deposited on different titania samples. The surface areas of

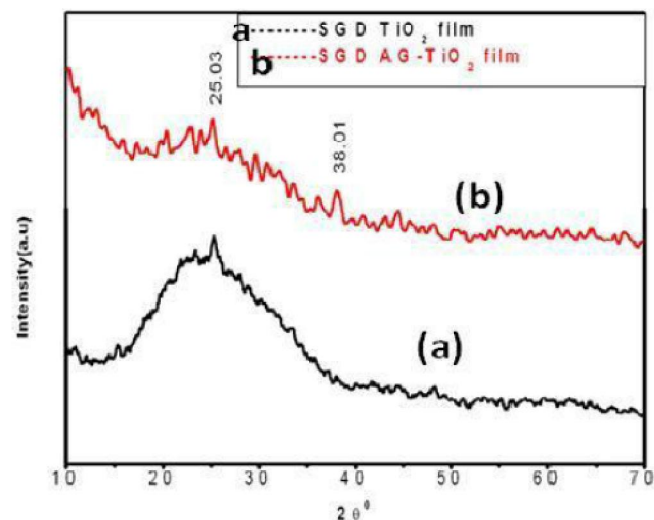


Figure 1b : Typical XRD pattern of (a) TiO₂ and (b) Ag-TiO₂ nano films prepared by SGD technique

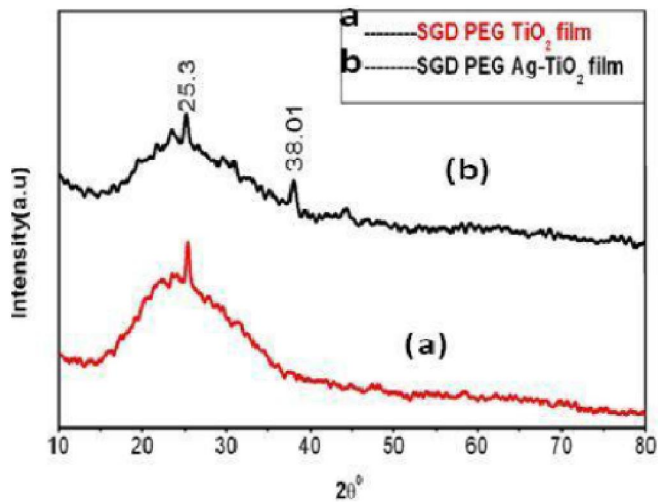


Figure 1c : XRD pattern of (a) TiO_2 and (b) Ag-TiO_2 nano films prepared by SGD surfactant PEG -2000

EBE Ag-TiO_2 , SGD Ag-TiO_2 , and PEG- SGD Ag-TiO_2 are much higher than that of different titania samples i.e. The crystallite size of composite film obtained by EBE evaporated was estimated to be about 24.8 nm, while the crystallite size grown by

without surfactant SGD film was in the range of 23.75 nm and crystallite size grown by PEG-2000 surfactant SGD film was around 9.8 nm Thus, PEG-2000 surfactant SGD film has larger surface area as compared to those of other technique, which in turn affects the catalytic activity.

SEM analysis of TiO_2 and Ag-TiO_2 nano thin films

SEM images of pure TiO_2 and the composite films with different silver content are presented in Figure 2.a to 2.f. While all TiO_2 films were sintered at 500°C , the morphology of constituted grains seems to be different depending on Ag content. The image of pure EBE and SGD TiO_2 films illustrates an extremely smooth, dense surface and there are no defects were observed (Figure 2.a - 2 b).

On the other hand, it deserves to be mentioned that the pore-forming process was ascribed to the presence of PEG surfactant. It was reported that surfactant PEG amount was lower than 0.0025 M, small cracks on the surface that would easily disappear

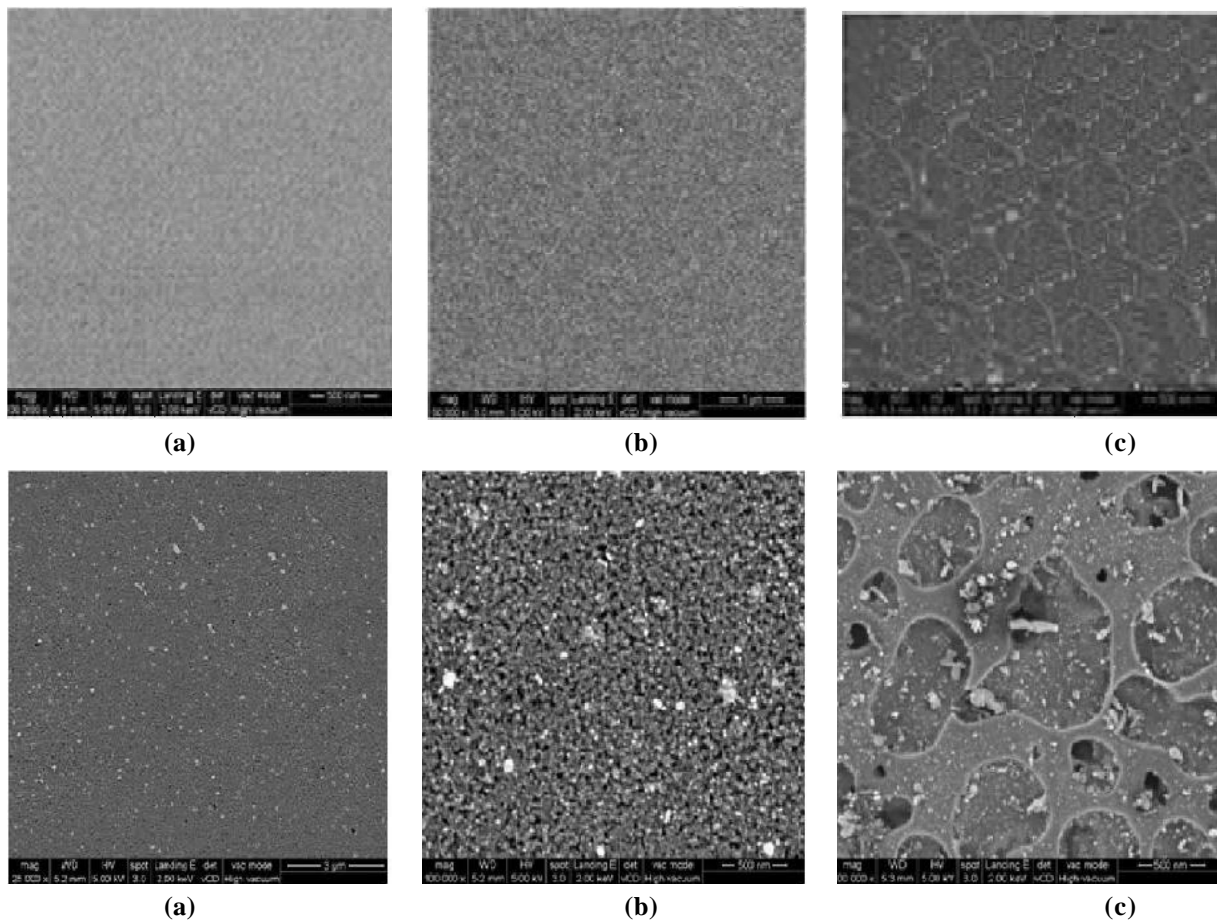


Figure 2 : SEM images of TiO_2 and Ag-TiO_2 thin films

Full Paper

since TiO₂ grain size was enlarged in the TiO₂ film during thermal treatment. This indicated, as anticipated, that TiO₂ colloidal particles were absorbed on same PEG chains. If PEG content in TiO₂ sols was lower than the critical value (0.002–0.0025 M), than colloidal particles cannot be coated by PEG and serious agglomeration among particles occurs over the period of thermal treatment. In contrast, PEG molecules were absorbed on same TiO₂ particle surface when PEG amount was higher than critical value (Figure 2.c), which supports that TiO₂ colloidal particles did not easily agglomerate due to the steric hindrance of PEG molecular chains. In this case, PEG molecules therefore would not contribute to a complete enlargement of aperture, and the shape of holes would become irregular and fluctuating as the content of PEG continued to increase up to 0.05 M, which was shown in Figure 2c.

Considering that heavy elements (eg. Ag) back-scatter electrons more strongly than light elements (e.g. O, Ti), the metallic silver appears brighter in the image. At low AgNO₃ concentrations, the shining Ag nanoparticles with a diameter around 20–30 nm were well dispersed as shown in Figure 2 (d) and 2. (e). The surface of without surfactant assisted TiO₂ film is different to that of surfactant assisted TiO₂ film. The density of Ag nanoparticles was increased with respect to surfactant TiO₂ film due to mass fraction of Ag which is 9.04% and the mass fraction of Ag in without surfactant Ag-TiO₂ is 1.33% for glycol reduction method. Further from SEM images it is clear that, no obvious aggregation was observed on the surface of TiO₂ films (see in Figure 2d and 2e). Although the size of the silver particles is smaller with diameter around 10 nm, there are no pores detected in the Ag-TiO₂ thin film without surfactant, whereas surfactant assisted Ag-TiO₂ films detected more nanopores and excess Ag⁺ ions which would gradually migrate along with the anatase grain boundaries to surface of the TiO₂ film during the Mw- irradiation process, whereas TiO₂ anatase grains thereby was depressed and specific surface area increases. In Figure 2f. shows larger Ag nanoparticles distributed on the surfactant TiO₂ films. Finally, Ag⁺ ions probably exist on the surface of the anatase grains by forming Ag–O–Ti bonds. The

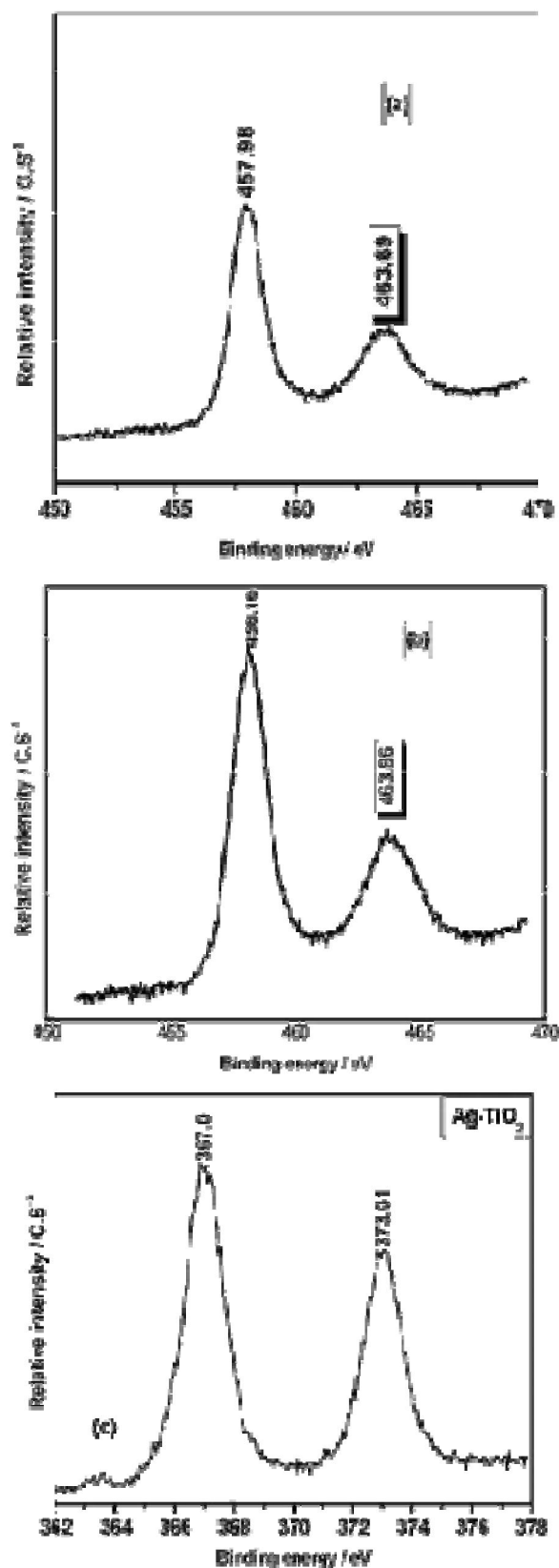


Figure 3 : (a) XPS survey scan of Ti_{2p} in TiO₂ film (b) XPS survey scan of the Ti_{2p} in mol % Ag-TiO₂ (c) XPS survey scan of Ag_{3d} in Ag-TiO₂ film

porous feature of the film indicates that it should have a rough surface as shown in Figure 2f.

XPS spectral studies of EBE TiO₂ and Ag-TiO₂ films

To determine the composition of films and identify the valence states of various atoms present, XPS analyses were carried out and the spectra's are shown in Figure 3. First, a wide scan survey spectrum was taken to determine elements present in each sample and then windows were recorded for each constituent (titanium, silver, oxygen) in a multiscan recording mode with a resolution of 1.2 eV. No trace of any impurity has been observed in the film except for a small amount of carbon. The highly symmetric shapes of titanium XPS lines clearly indicate that the titanium is present only as Ti⁴⁺. In fact, the presence of titanium having an oxidation state lower than + 4 should have been evidenced by presence of shoulders on lower binding energy side of the peak, which was not observed. Moreover, the binding energy of Ti 2p_{3/2} line is found at 458.5 eV and 463.86 eV, respectively which matches well with in literature values, after subtracting the C_{1s} line with the obtained values these charging effect is taken into account. These results and, as well as the difference in binding energies between Ti 2p_{3/2} and O_{1s} lines, are in good agreement with the studies performed on single crystalline TiO₂ (110) surfaces prepared by electron beam evaporation technique.

The signals of Ag in EBE Ag-TiO₂ samples are

shown in Figure 3.b. It is found that binding energies of Ag 3d at about 367.0 and 373.01 eV on Ag-TiO₂ should be assigned to 3d_{5/2} and 3d_{3/2}, respectively. These data exhibit a negative shift compared to those of bulk Ag (368.3 eV for 3d_{5/2} and 374.3 eV for 3d_{3/2})^[42], probably suggesting that some electrons may transfer from TiO₂ to metallic Ag and there is strong interaction between Ag particles and TiO₂ support. Jingxia^[43] obtained similar signals of Ag in Ag-TiO₂ samples deposited by chemical deposition technique. As it is known that the Fermi level of Ag is lower than that of TiO₂, the conduction band electrons of TiO₂ may transfer to deposited Ag on the surface of TiO₂, resulting in an increase in the outer electron cloud density of Ag nanoparticles.

EDS elemental analysis

From elemental mapping results, it can be seen that the three elements, Ag, Ti and O, are distributed evenly throughout the nanocomposite. X-ray energy dispersive spectroscopic (EDS) analysis indicated that nanocomposite consisted mainly of Ag, Ti, and O (Figure 4a and 4b). The spectrum (Figure 4a) of surfactant Ag-TiO₂ nanocomposite shows two satellite peaks at 2.983 eV and 3.149 eV, due to multi-electron processing of Ag atom (i.e. electron repulsion). The spectrum in Figure 4.b of SGD Ag-TiO₂ nanocomposite indicated that only one peak of Ag metal occurred at 2.984 eV. Similarly, Ti displayed a major satellite peak occurred at 4.510 eV and Si most likely originate from glass substrate.

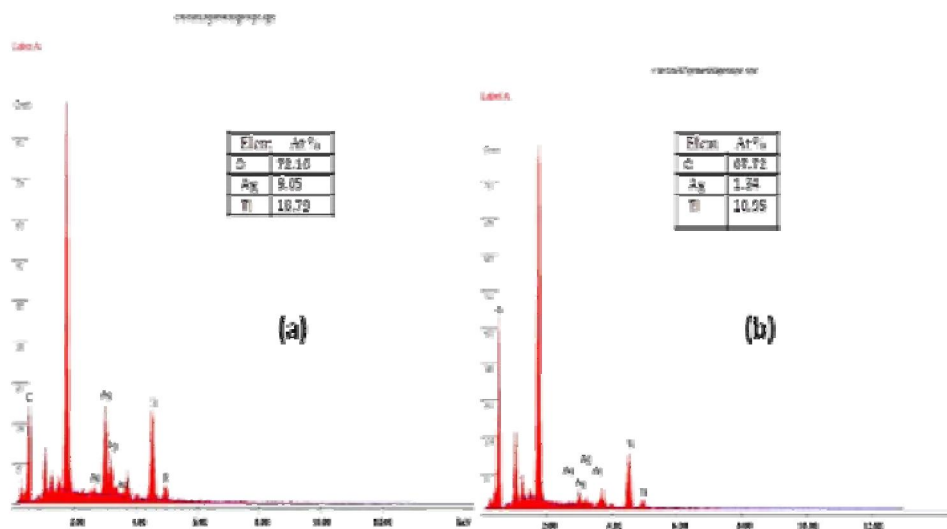


Figure 4 : EDS analysis of (a) SGD-PEG Ag-TiO₂ and (b) SGD Ag-TiO₂ nanocomposites

Full Paper

UV-Visible absorption spectral studies

UV-Visible absorption spectroscopy

Figure 5[A] shows that UV-Vis absorption spectra of pure EBE TiO₂ and Ag ion-implanted on EBE TiO₂ films deposited on glass substrate. The pure EBE TiO₂ can only have an absorption range less than 331 nm. The color of EBE TiO₂ film appeared in the wavelength range 350–800 nm due to interference bands. After implantation of Ag ion, the absorption rate increased and small amount of absorption wavelength shifts towards longer wavelength. The influence of metal ion implantation on the near-surface microstructure and chemistry resulted mainly from combined ion mixing and alloying effects. This shift can be ascribed due to extra Ag impurity energy level with in the band gap such results indicate that the method of doping causes electronic properties of titanium oxides to be modified in completely different ways, thus confirming that only metal ion-implanted titanium oxide show shifts in absorption band towards visible light regions.

In Figure [5B] shows that absorbance spectrum of surfactant, without surfactant TiO₂ and Ag-TiO₂ films. It is distinctly observed that overall absorbance has markedly increased due to the incorporation of Ag NPs. This observation may be of critical impact to photophysical areas of research including visible light photocatalytic activity or photovoltaic

applications. One of the major objectives of incorporation of Ag nanoparticles into surfactant and without surfactant TiO₂ nanoparticles is to increase the wavelength response range in order to enhance the photo excitation efficiency of TiO₂. But with the experimental result Plasmon peak moves to lower wavelengths on doping of TiO₂ thin films indicates that particle size decreases with doping of Ag content. Also, the optical properties such as band gap of Ag-TiO₂ and TiO₂ nano film were determined by Tauc's plot method^[19]. The indirect band gap value reported in literature for bulk and film anatase is estimated at 3.2 eV of EBE TiO₂ film. The larger band gap of the obtained SGD TiO₂ films in comparison to their bulk values is presumably due to the lattice deformation by an axial strain of these films^[20]. The evaluated band gap for undoped SGD TiO₂ films has given in TABLE 1. which is comparable to the values (3.7eV) cited in the literature which is due to quantum dot anatase TiO₂ thin films^[21]. correspondingly, the absorbance edge of SGD Ag-TiO₂ films shifts significantly to lower wavelength as compared to that of SGD TiO₂ nano thin films this as shown in Figure 5[B] (curve e, f)., it is interesting to note here that while there is no significant absorption in the undoped TiO₂ for energies below its band gap, there is considerable absorption in Ag-doped samples in the lower energy region (2.1–3.66 eV), increasing almost linearly with increasing energy.

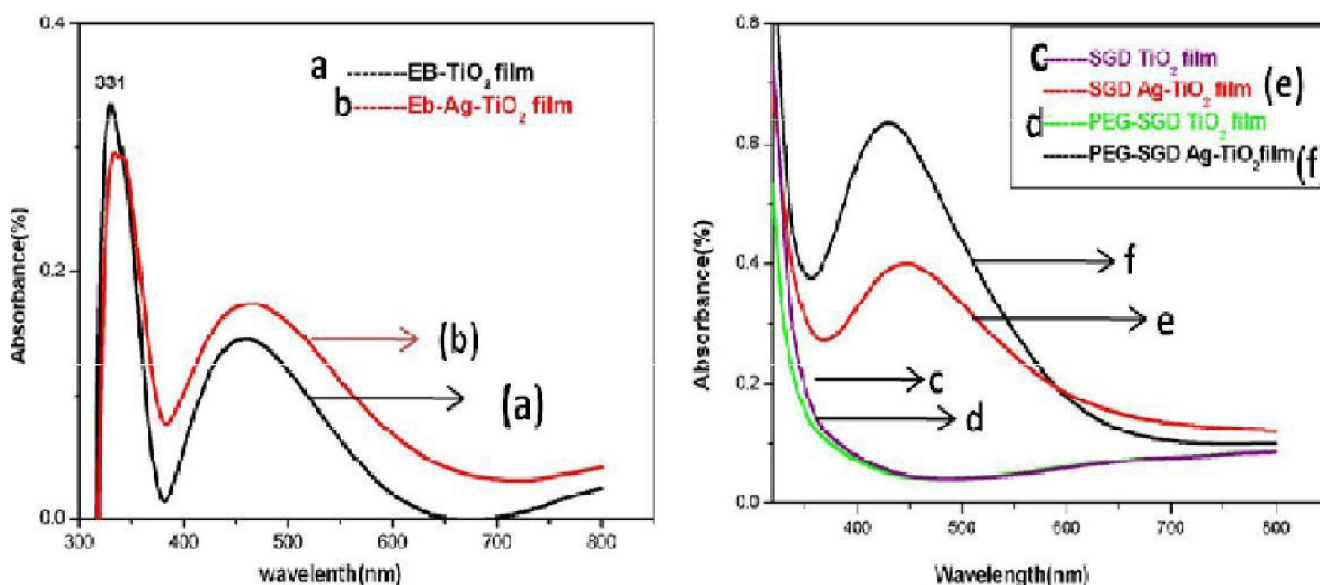


Figure 5 : UV-Visible absorbance spectra's of TiO₂ and Ag-TiO₂ films

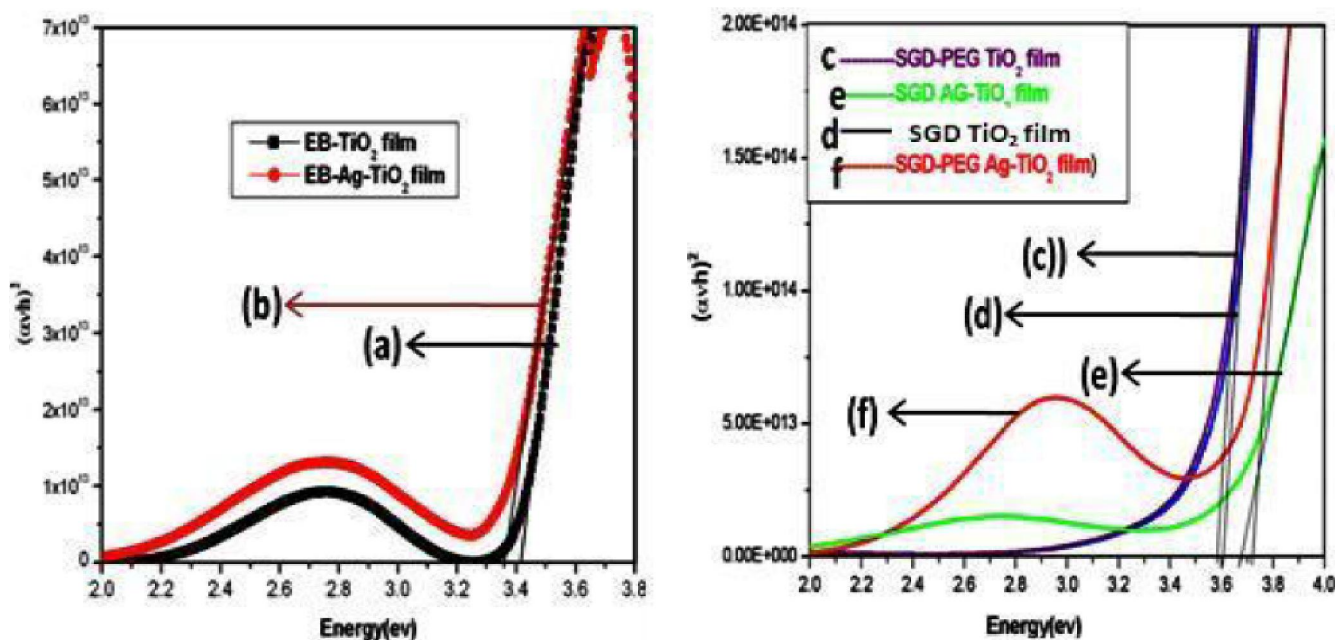


Figure 6 : Plot of $(\alpha h\nu)^2$ as a function of photon energy (eV) for TiO_2 and Ag- TiO_2 films

The surface plasmon absorption band of metal nanoparticles can be influenced by many factors such as particle size, particle shape, particle size distribution, surface charge density etc. Also, the surface plasmon absorption peak became broader and moves towards longer wavelengths when the size of nanoparticle is increased as compared to surfactant Ag- TiO_2 films. The increase in size distribution which leads to broadening of surface plasmon absorption peak^[44]. It can be seen from Figure 5[B] (e and f) shows that surface plasmon absorption peak became broader with the increasing of Ag content and shifts the wavelength towards shorter region due to quantum dot effect.

Photocatalytic activity test

Figure 7[A] shows that photo-catalytic activities of 500°C calcinated TiO_2 films prepared by EBE gun and SGD methods. A very small percentage of methylene blue decomposes in the absence of semi-conducting oxide films. It is seen that about 51% of methylene blue was decomposed after UV illumination for 2.5 h in case of TiO_2 -EBE films, whereas 60-77% methylene blue was decomposed after 2.5 h using without surfactant and surfactant SGD TiO_2 films. Therefore, it can be compared from the obtained result that SGD films are superior photoactivity then EBE films. This decline in the

photocatalytic activities can be linked with following two facts.

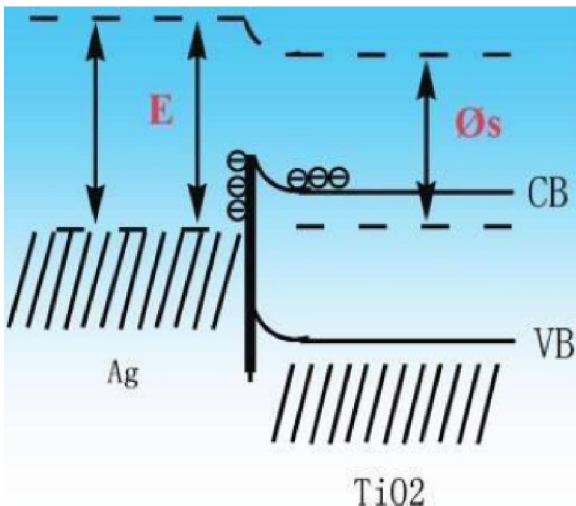
The possible reason for increasing the photocatalytic activity of SGD TiO_2 films is mainly due to Ti^{3+} ions are formed during calcination as a result of reduction of Ti^{4+} to Ti^{3+} by organic residues, such as alcohol and unhydrolyzed alkoxide group. Organic residuals draw oxygen atoms from surrounding TiO_2 network. Ti^{3+} ions on the surface of TiO_2 films may trap the photogenerated electrons, which are transferred from Ti^{3+} surface states to O_2 adsorbed on active sites of Ti^{3+} . This results in the reduction of recombination of Photogenerated electrons and holes. The formation of a larger amount of Ti^{3+} ions contributes largely to the enhancement of the photoactivity of TiO_2 films^[45, 46]. On the other hand, Ti^{3+} ions may not form in the case of the EBE films. Jiang et al.^[47] found that oxygen concentration in EBE TiO_2 films is homogeneous and that if the oxygen pressure is higher than 1.6×10^{-4} Torr, the stoichiometric ratio of O to Ti in EBE films is consistent with the normal value of TiO_2 .

It can be observed that efficiency of degrading MB increases with increasing number of layers of SGD PEG- TiO_2 film is as shown in Figure 7a. This result can be explained by assuming that in layered by layered films the electrons can travel further before returning to the surface of the semiconductor,

Full Paper

TABLE 1 : The band gap of TiO₂ and Ag-TiO₂ photocatalyst prepared by different techniques

Films	Band gap(eV)		
	With surfactant	Without surfactant	EBE
Ag-TiO ₂	3.7	3.68	3.35
TiO ₂	3.6	3.58	3.4

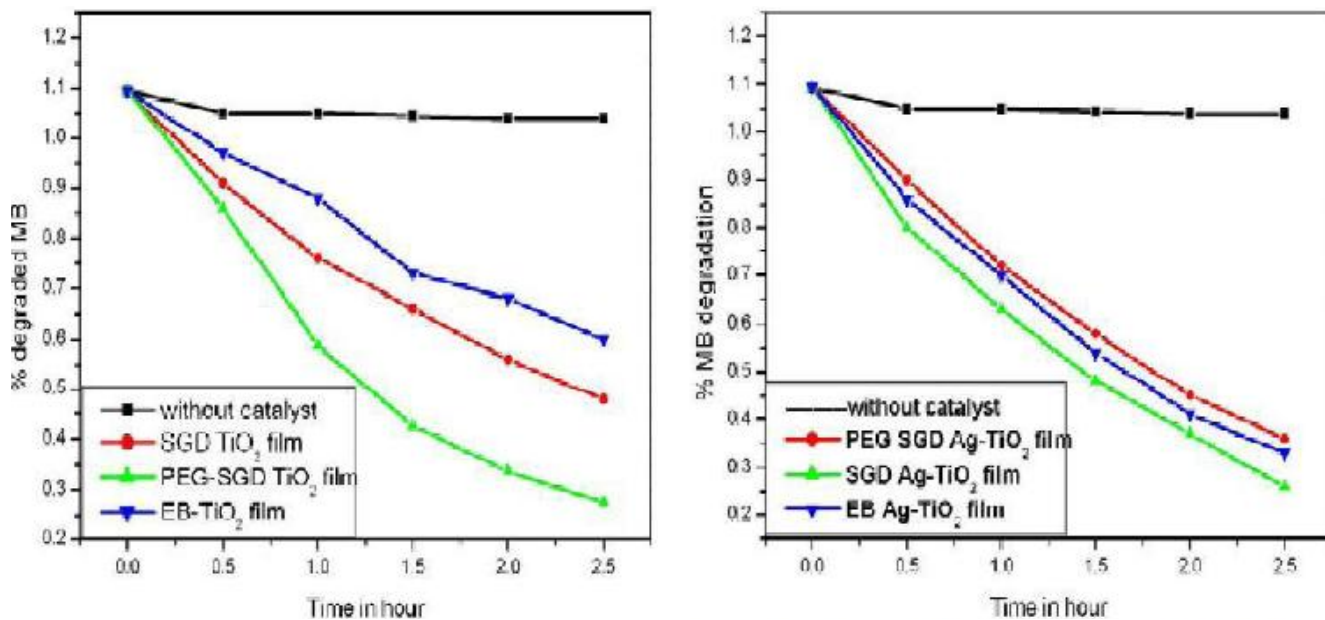
Scheme 1 : Schematic photocatalytic mechanism of Ag-TiO₂ film

making the recombination process slower and implying higher photocatalytic efficiency, owing to a greater density of h⁺ at the surface. In single layered film, this effect is too fast, due to the shorter electron path, resulting in a lower efficiency. Thus, in case of SGD PEG-TiO₂ film increases the photocatalytic activity due to inhibition of recombination

electron-hole pairs and porous nature of the material.

Silver nanoparticles plays important role when deposited on TiO₂ surface, which could act as electron-hole separation centers^[48-50]. As shown In Sheme.1, the fermi level of TiO₂ was higher than that of silver, Therefore photo-generated electrons were transferred from the TiO₂ conduction band to metallic silver particles and clusters spreading on the TiO₂ film resulting in a space charge layer at the boundaries between Ag and TiO₂. Moreover, as shown in Figure 7b, it is obvious that SGD Ag-TiO₂ shows the highest photocatalytic activity among the other Ag-TiO₂ samples and photocatalytic performance of all the three Ag-TiO₂ samples as shown in the following order: SGD Ag-TiO₂ > EBE Ag-TiO₂ > SGD PEG Ag-TiO₂. This conclusion can be explained from the following considerations.

1. From the Xps data of EBE Ag-TiO₂ films shows that strong interaction between surface Ag nanoparticles and TiO₂ will effectively inhibit the recombination of excited electrons and holes, which

Figure 7 : Photocatalytic degradation of methylene blue using (a) TiO₂ and (b) Ag-TiO₂ thin films

increase the photocatalytic performance of EBE Ag-TiO₂ films than the EBE TiO₂ films.

2. It should be noted that 9.37 mol% Ag particles and clusters occurring on SGD PEG- TiO₂ film are relatively negatively charged, holes in the interfacial region of TiO₂ film may be trapped by these Ag particles and clusters before they react with surface hydroxyl groups and water. As in case of without surfactant Ag-TiO₂ film the silver concentration is 1.37%, it seems that the trapping effect is neglectable, whereas Ag particles and clusters principally promotes the TiO₂ charge separation efficiency, hence same charge pair separation and preventing their recombination. About 74.5% percentage of methylene blue decompose in the presence of unsurfactant Ag-TiO₂ films, whereas 64 % of methylene blue decomposed after UV illumination for 2.5 h by using surfactant Ag-TiO₂ films because of excess Ag content on oxide films, which also act as a trapping site by accepting the photo excited electrons from the TiO₂ valence band. The Scheme 1 illustrates a mechanistic diagram of silver nanoparticle effect on TiO₂ films as shown below.

CONCLUSION

In this work we have investigated the effect of Ag doping on photocatalytic activity of TiO₂ films prepared by microwave glycol reduction process. It was found that with a suitable percentage of Ag dopant (1.37%), effectively increases the photocatalytic activity. This fact can be explained by increase in the electron-hole separation efficiency induced by enhancing the charge pair separation and inhibiting their recombination by adding the Ag dopant. From the obtained result surfactant Ag-TiO₂ samples demonstrate lower photocatalytic activity than without surfactant Ag-TiO₂ samples which is due to excess silver deposition on TiO₂ films, i.e. It will act as a trapping site by accepting the photo excited electrons from TiO₂ valence band. Also it can be concluded that synthesis of nanostructured TiO₂ films by polymeric precursor method was effective for degradation of methylene blue dye because of layer by layer increases the thickness, porosity and inhibiting the recombination of electron-hole pair which

supports to increase the photocatalytic activity.

REFERENCES

- [1] M.Formenti, F.Juillet, P.Meriaudeau, S.J.Teichner; *Chem.Technol.*, **1**, 680-686 (1971).
- [2] A.Fujishima, K.Honda; *Nature.*, **238**, 37-38 (1972).
- [3] O.Carp, C.L.Huisman, A.Reller; *Prog.Solid State Chem.*, **32**, 33-177 (2004).
- [4] J.M.Herrmann; *Catal.Today*, **53**, 115-129 (1999).
- [5] M.R.Hoffmann, S.T.Martin, W.Choi, D.W.Bahnmann; *Chem.Rev.*, **95**, 69-96 (1995).
- [6] A.L.Linsebigler, G.Lu, J.T.Yates; *Chem.Rev.*, **95**, 735-758 (1995).
- [7] A.Mills, S.Le Hunte; *J.Photochem.Photobiol.A*, **108**, 1-35 (1997).
- [8] A.Fujishima, T.N.Rao, D.A.Tryk; *J.Photochem.Photobiol.C*, **1**, 1-21 (2000).
- [9] A.Fujishima, X.T.Zhang; *C.R.Chim.*, **9**, 750-760 (2006).
- [10] A.A.Adesina; *Catal.Surv.Asia.*, **8**, 265-273 (2004).
- [11] A.Mills, S.K.Lee; *J.Photochem.Photobiol.A.*, **152**, 233-247 (2002).
- [12] S.Malato, J.Blanco, A.Vidal, D.Alarcon, M.I.Maldonado, J.Caceres, W.Gernjak; *Sol.Energy*, **75**, 329-336 (2003).
- [13] M.Romero, J.Blanco, B.Sanchez, A.Vidal, S.Malato, A.Cardonaand E.Garcia; *Sol.Energy*, **66**, 169-182 (1999).
- [14] M.Kitano, M.Matsuoka, M.Ueshima M.Anpo; *Appl.Catal.A.*, **325**, 1-14 (2007).
- [15] T.L.Thompson, J.T.Yates; *Chem.Rev.*, **106**, 4428-4453 (2006).
- [16] M.Anpo; *Pure Appl Chem.*, **72**, 1787-1792 (2000).
- [17] M.D.H.A.Fuerte, A.J.Maira, A.Martinez Arias, M.Fernandez Garcia, J.C.Conesa, J.Soria; *Chem Commun.*, **24**, 2718-2719 (2001).
- [18] H.Yamashita, M.Harada, J.Misaka; *J.Synchrotron Rad.*, **8**, 569-571 (2001).
- [19] T.Ihara, M.Miyoshi, M.Ando, S.Sugihara, Y.Iriyama; *J.Mater Sci.*, **36**, 4201-4207 (2001).
- [20] K.Takeuchi, I.Nakamura, O.Matsumoto, S.Sugihara, M.Ando, T.Ihara; *Chem Lett.*, **29**, 1354-1355 (2000).
- [21] T.Ohno, T.Mitsui, M.Matsumura; *Chem Lett.*, **32**, 364-365 (2003).
- [22] Y.Liu, X.Chen, J.Li, C.Burda; *Chemosphere*, **61**, 11-18 (2005).
- [23] J.C.Yu, L.Zhang, Z.Zheng, J.Zhao; *Chem Mater.*, **15**, 2280-2286 (2003).

Full Paper

- [24] T.Hirai, K.Suzuki, I.Komasawa; *J.Colloid Interface Sci.*, **244**, 262-265 (2001).
- [25] H.Zhang, G.Chen, D.W.Bahnmemann; *J.Mater.Chem.*, **19**, 5089-5121 (2009).
- [26] H.Tada, T.Kiyonaga, S.Naya; *Chem.Soc.Rev.*, **38**, 1849-1858 (2009).
- [27] J.Y.Lan, X.M.Zhou, G.Liu, J.G.Yu, J.C.Zhang, L.J.Zhi, G.J.Nie; *Nanoscale*, **3**, 5161-5167 (2011).
- [28] (a) S.Naya, M.Teranishi, T.Isobe, H.Tada; *Chem.Commun.*, **46**, 815-817 (2010).
- [29] S.Link, M.A.El Sayed; *J.Phys.Chem.B.*, **103**, 8410-8426 (1999).
- [30] M.Kerker; *J Colloid Interface Sci.*, **105**, 297-314 (1985).
- [31] D.D.Evanoff, G.Chumanov; *Chem Phys Chem.*, **6**, 1221-1231 (2005).
- [32] Z.Ding, X.Hu, P.L.Yue, G.Q.Lu, P.F.Green eld; *Catal.Today*, **68**, 173-182 (2001).
- [33] R.S.Sonawane, S.G.Hegde, M.K.Dongare; *Mater.Chem.Phys.*, **77**, 744-750 (2002).
- [34] H.K.Pulker, G.Paesold, E.Ritter; *Applied Optics.*, **15**, 2986-2991 (1976).
- [35] N.Smirnova, V.Vorobets, O.Linnik, E.Manuilov, G.Kolbasov; *Surf.Interface Anal.*, **6**, 1205-1208 (2010).
- [36] Feng Peng, Hancai Zhu, Hongjuan Wang, HaoYu, Korean; *J.Chem.Eng.*, **24**, 1022-1026 (2007).
- [37] Enrico Traversa, maria luisa di vona, Patrizia nunziante, Silvia; *Journal of Sol-Gel Science and Technology.*, **19**, 733-736 (2000).
- [38] Bin Zhao, YuWen Chenan; *J.Physics and Chemistry of Solids*, **72**, 1312-1316 (2011).
- [39] Xiaobin Li, Linling Wang, Xiaohua Lu; *Journal of Hazardous Mat.*, **177**, 639-647 (2010).
- [40] M.Vishwas, Sudhir Kumar Sharma, K.Narasimharao, S.Mohan, K.V.Arjuna Gowda, R.P.S.Charkradhar; *Spectrochimica Act.*, **75**, 1073-1077 (2010).
- [41] Feng Lajun, Guo Meijuan, Feng Hui; *Journal of Functional Mat.*, **43**, 2002-2006 (2012).
- [42] J.F.Moudler, W.F.Stickle, P.E.Sobol, K.D.Bomben; *Handbook of X-ray photoelectron spectroscopy*, Perkin-Elmer: Eden, (1992).
- [43] Jingxia Li, Jianhua Xu, Wei-Lin Dai, Kangnian Fan; *J.Phys.Chem.C*, **113**, 8343-8349 (2009).
- [44] J.Yu, J.Xiong, B.Cheng, S.Liu; *Appl.Catal.B*, **60**, 211-221 (2005).
- [45] I.Sopyan, M.Watanabe, S.Murasawa, K.Hashimoto, A.Fujishima; *J.Photochem.Photobiol.*, **A**, **98**, 79-86 (1996).
- [46] L.Hu, T.Yoko, H.Kozuka, S.Sakka; *Thin Solid Films*, **219**, 18-23 (1992).
- [47] J.C.Jiang, H.S.Cheng, B.Li, Z.H.Wang, Z.Q.Zhang, F.S.Zhang, F.J.Yang; *Nucl.Instrum.Methods*, **B**, **190**, 514-517 (2002).
- [48] J.Herrmann, J.Disdier, P.Pichat; *J.Phys.Chem.*, **90**, 6028-6034 (1986).
- [49] A.Henglein; *J.Phys.Chem.*, **83**, 2209-2216 (1979).
- [50] J.M.Herrmann, R.T.K.Baker, S.J.Tauster, J.A.Dumesic; *ACS Symposium Series*, **298**, 200-211 (1986).